Direct observation and quantification of nanosecond laser induced amorphization inside silicon \odot

Xinya Wang ^⑤; Lanh Trinh ^⑥; Xiaoming Yu ^⑥; Matthew J. Berg ^⑥; Sajed Hosseini-Zavareh; Brice Lacroix; Pingping Chen ^⑥; Ruqi Chen ^⑥; Bai Cui ^⑥; Shuting Lei [☑] ^⑥



J. Laser Appl. 36, 022015 (2024) https://doi.org/10.2351/7.0001305









Direct observation and quantification of nanosecond laser induced amorphization inside silicon

Cite as: J. Laser Appl. 36, 022015 (2024); doi: 10.2351/7.0001305 Submitted: 10 December 2023 · Accepted: 3 March 2024 · Published Online: 27 March 2024







Xinya Wang,¹ 🔟 Lanh Trinh,² 🗓 Xiaoming Yu,³ 🗓 Matthew J. Berg,⁴ 🔟 Sajed Hosseini-Zavareh,⁴ Brice Lacroix,⁵

AFFILIATIONS

- Department of Industrial and Manufacturing Systems Engineering, Kansas State University, Manhattan, Kansas 66506
- ²Department of Mechanical and Materials Engineering, University of Nebraska-Lincoln, Lincoln, Nebraska 68588
- ³The College of Optics and Photonics, University of Central Florida, Orlando, Florida 32816
- ⁴Department of Physics, Kansas State University, Manhattan, Kansas 66506
- Department of Geology, Kansas State University, Manhattan, Kansas 66506

ABSTRACT

tron microscopy measurements of cross sections of the modified channels reveal highly localized crystal deformation. Raman spectroscopy measurements prove the existence of amorphous silicon inside nanosecond laser induced modifications, and the percentage of silicon is calculated based on the Raman spectrum. For the first time of the show the appearance of amorphous silicon inside nanosecond laser induced modifications, which corroborates the indirect measurements from Raman spectroscopy. The laser modified channel consists of a small amount of amorphous silicon embedded in a disturbed crystal structure accompanied by strain. This finding may explain the origin of the positive refractive index change associated with the written channels that may serve as optical waveguides.

Key words: laser modification inside silicon, ns laser, amorphous silicon, Raman analysis, HRTEM imaging

Published under an exclusive license by Laser Institute of America. https://doi.org/10.2351/7.0001305

I. INTRODUCTION

Silicon is the basic semiconductor material for numerous applications, such as sensors, photovoltaics, optoelectronics, MEMS devices, and microelectronics. One of the major needs in today's communications industry is to integrate electronic and photonic devices on the same chip. 1,2 Direct writing of optical waveguides using ultrashort laser pulses is a promising approach to achieve this goal.^{2–5} However, direct writing inside silicon has several difficulties compared to writing inside glass or other dielectrics, such as strong spherical aberration and nonlinear interactions.⁵

Countless methods have been attempted to overcome these limitations since 1990s. 6-15 Localized modifications in the bulk of silicon induced by 3.5 ns laser pulses have been reported.⁴ The properties of the internal modifications generated by nanosecond laser pulses have been investigated. 4-7 Longitudinally written waveguides inside silicon by nanosecond laser has been presented.8 Direct writing of single-mode waveguides in Si with picosecond (ps) laser pulses has been reported.9 Waveguides have been written by femtosecond (fs) pulses at the interface of $\mathrm{SiO}_{2}/\mathrm{Si.}^{3}$ Waveguides deep inside bulk Si with 350 fs laser pulses at a wavelength of 1550 nm have been demonstrated. Local modification in the bulk of Si with sub-100-fs laser pulses has also been proved by tight focusing at the center of silicon spheres using an extreme solid-immersion technique. 12 Depressed-cladding waveguides inside bulk silicon written by nanosecond laser pulses have been demonstrated to be feasible.¹

a) Author to whom correspondence should be addressed; electronic mail: lei@ksu.edu

Both straight and curved waveguides have been written inside silicon by transverse ns laser writing. 14,1

The past decades have seen achievements in the field of laser induced modifications and waveguide writing inside silicon; however, many problems still remain to be solved. 16-20 One problem is related to the structural changes of the modifications inside silicon induced by a pulsed laser. When laser pulses, especially ultrashort pulses, are focused inside silicon, the extremely high temperature and pressure at the focusing spot often result in complicated material changes, such as melting, explosion, shock wave, and re-solidification. Past research has shown many different material changes inside silicon induced by pulsed lasers, including voids, 16,17 high-pressure phases, 18 dislocations, 7,19 hydrostatic compressive strain, 7,19 cracks, 16 and polycrystalline features. 10,18,20 Another problem is concerned with the light-guiding mechanism of the waveguides created inside silicon. The origin of the positive refractive index change associated with the written waveguides calls for further investigation.²⁰ Given the fact that the refractive index of amorphous silicon ($n_{a-Si} = 3.73$) is higher than that of crystalline silicon ($n_{c-Si} = 3.48$ at 1.55- μ m wavelength), we may expect a partial amorphization of silicon for explaining the waveguiding abilities.²⁰ However, there has been no direct evidence showing the amorphous silicon inside nanosecond laser induced modifications and waveguides. Thus, a better understanding of the material changes inside ns laser induced modifications is important to provide guidance for the next generation of silicon devices. It is critical to understand the light guiding mechanisms of waveguides written inside silicon and make low-loss waveguides possible.

In this paper, we investigate the structural changes of ns-laser written channel modifications in silicon by means of Raman microscopy and TEM. Our focus is to search for laser induced amorphization of silicon through HRTEM and quantify the amorphous silicon in the modified zone using Raman spectroscopy. Scientifically, it can answer questions such as whether and how much amorphization occurs under ns laser irradiation inside silicon, which should stimulate further investigations on the mechanisms of laser induced amorphization as well as the reason for the location and quantity of amorphous silicon in the modified zone. Such insights gained about laser induced amorphization of silicon will potentially help engineer the refractive index change to enable low-loss waveguides written inside silicon for applications in integrated optoelectronic devices. Our Raman results prove the existence of amorphous silicon inside laser induced modifications, and the percentage of amorphous silicon is calculated based on the Raman spectrum. For the first time, the HRTEM images directly show the appearance of amorphous silicon inside ns-laser induced modifications. Such amorphous silicon may be responsible for a positive refractive index change in the range of 10^{-3} .

II. EXPERIMENTAL PROCEDURE

The experimental setup for the laser modification inside silicon is shown in Fig. 1. The laser is a fiber MOPA (master oscillator power amplifier) laser (MWTechnologies, Model PFL-1550) delivering laser pulses at 1.55 µm center wavelength and 3.5 ns FWHM (full-width-at-half-maximum) pulse duration. The pulse repetition rate is 20–150 kHz and the pulse energy is 20 μJ. During

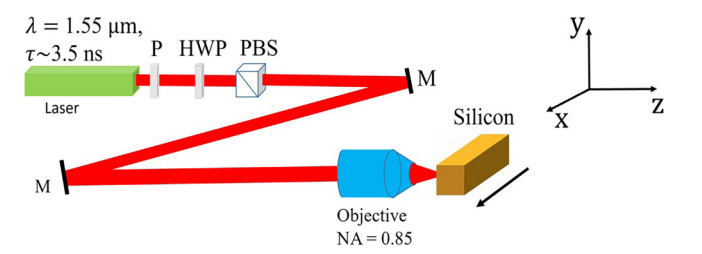


FIG. 1. Experimental setup for transverse ns laser writing inside silicon. P: polarizer. The combination of half-wave plate (HWP) and polarizing beam splitter (PBS) are used to tune the power. The numerical aperture (NA) of the objective lens is 0.85.

laser writing, a spherical aberration corrected objective lens (Olympus, LCPLN100XIR, NA = 0.85) is used to focus the beam into the silicon sample. The focal spot diameter at $1/e^2$ is $2w_0 = 2\lambda/(\pi NA) = 1.16 \,\mu\text{m}$, and the Rayleigh length is $Z_R = 2.6 \,\mu\text{m}$ in air and $z_R \approx 9.2 \,\mu\mathrm{m}$ in Si. The relative position between the sample and the objective lens is controlled using an XYZ translation stage (Newport, ILS100PP). The writing direction is perpendicular to the beam propagation axis. Based on our previous study,5-7,14,15 the following two writing conditions are selected for the sample preparation: (1) pulse energy $E = 10 \,\mu\text{J}$ and (2) $E = 6 \mu J$. The repetition rate is fixed at $f_p = 20 \text{ kHz}$ and the writing speed is fixed at V = 1 mm/s. After laser inscription, the sample is cleaved to observe the cross section of the channel modification by an optical microscope.

In order to investigate the origin of the laser induced refractive index change, Raman spectroscopy is used to determine the composition of the modification. Raman microscopy is applied at a $\frac{1}{100}$ wavelength of 532 nm using a $100 \times$ objective with NA = 0.85(Renishaw inViaRaman microscope). 2D mappings are obtained by scanning with a step size of $2 \mu m$ in the x and y directions. The sample is cleaved perpendicular to the channel direction. The cross section of the channel is examined under the Raman microscope directly without further processing to avoid any further modification of the modified zone. The sample is characterized with a Raman microscope at three positions for every modification. In order to reveal the atomic scale microstructure of the modification, lamella samples are prepared from the modified zone using the focused ion beam (FIB) workstation (FEI, Helios 660 NanoLab) for TEM analysis. TEM characterizations including bright field imaging and HRTEM are carried out on an S/TEM system (FEI, Technai Osiris) operating at 200 kV.

III. RESULTS AND DISCUSSION

One can determine the ratio of the amorphous silicon in the modifications by the curve fitting of the Raman spectrum. In the case of silicon with mixed amorphous- monocrystalline phase composition, the spectrum includes a broad low-frequency component peaking around 480 cm⁻¹ which is from the amorphous phase, and a narrow peak near 520 cm⁻¹ which is from the crystalline phase.^{2,21} The total scattering intensity $I(\omega)$ in the frequency region

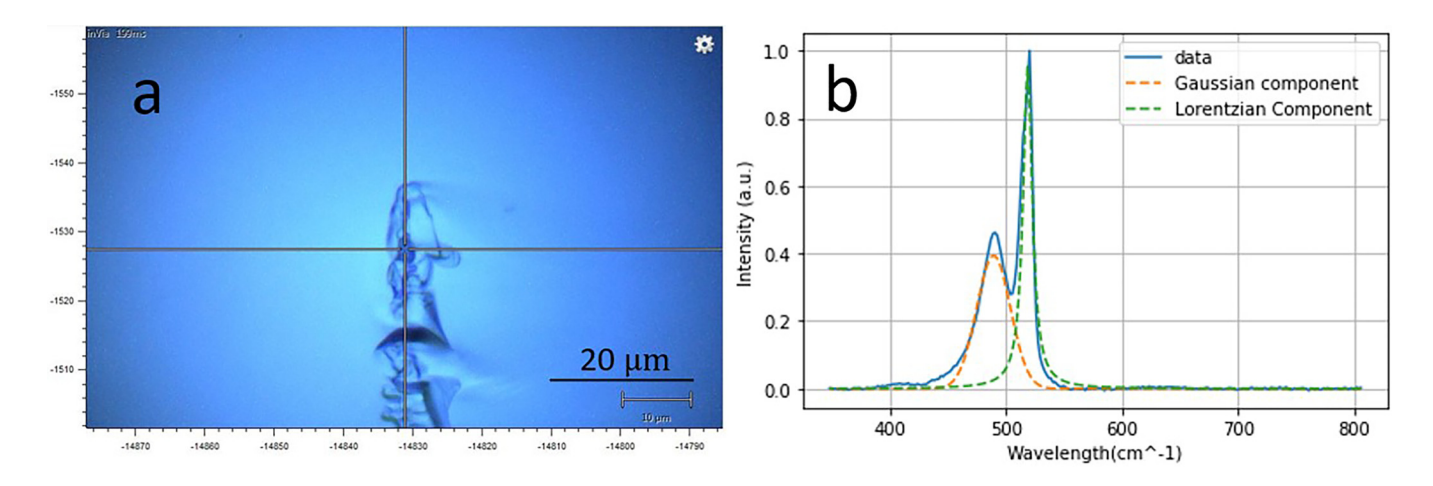


FIG. 2. (a) The laser modification inside silicon. (b) The Raman spectrum at the intersection of the two lines in (a). The solid curve is the original data, the left dashed curve is the Gaussian fit (amorphous silicon), and the right dashed curve is the Lorentzian fit (monocrystalline silicon).

can be written as

$$I(\omega) = I_c(\omega) + I_a(\omega), \tag{1}$$

where $I_c(\omega)$ is the intensity of the line produced by the crystalline phase and $I_a(\omega)$ is that of the amorphous phase line.²

Based on the above theory, we wrote a program to analyze the percentage of the amorphous and crystalline silicon in the laser induced modifications. The analysis is done in python using a fitting module called non-linear least-squares minimization and curve-fitting for Python (Lmfit).²² The validity of the fitting program can be seen in Refs. 23–25. The amorphous component is represented by a Gaussian profile, while the crystalline component is represented by a Lorentzian profile.^{2,21} An optical image of the cross section of a laser modified zone is shown in Fig. 2, together with the Raman spectrum and the curve-fit Gaussian and Lorentzian components.

The modification in Fig. 2(a) is written with the pulse energy of 10 µJ, pulse repetition rate of 20 kHz, and scanning speed of 1 mm/s. The optical image shows that the modification is not uniform. A heavily modified part in the cross center is found, and the Raman spectrum from this position is analyzed by our in-house program. The results are shown in Fig. 2(b). The original Raman data (solid line) are split into two parts, the crystalline part (Lorentzian Component) and the amorphous part (Gaussian component). As an accuracy check, the areas underneath the fitting (28.73) and the experimental data (28.58) are very close (<1% in difference), as a result of small residuals between the measured data and the fit curves. This indicates that the area derived from the fit agrees with experimental data. As Fig. 2(b) indicates, the Lorentzian and Gaussian areas are calculated from the fitting. The Lorentzian contribution is (14.34 ± 0.4138) and the Gaussian area is (14.39 ± 0.4118) . The area underneath the Gaussian divided by the area underneath the whole curve indicates the amorphous ratio.

Based on our calculation, the percentage of amorphous silicon is 50.1% at this location.

To better understand the distribution of the amorphous silicon in the modified zone, 2D mapping of the Raman spectrum is done. Figure 3(a) shows the optical image of the modification written with the pulse energy of 6 µJ, pulse repetition rate of 20 kHz, and scanning speed of 1 mm/s. This cross-sectional view ≥ shows that the modification is elongated and non-uniform. The 2D mapping of the peak intensity at 480 cm⁻¹, an indication of amorphous silicon in the modified zone, is shown in Fig. 3(b). The 2D & mapping proves that amorphous silicon is created by ns laser writing, but it is non-uniform in the modified zone. There is a similarity between the Raman signal strength in Fig. 3(b) and the color

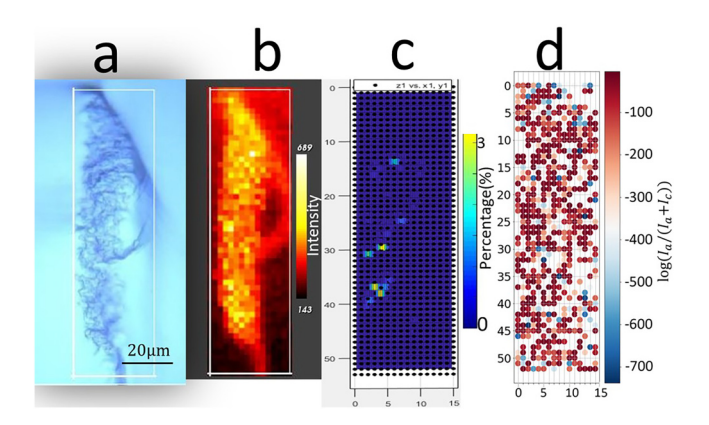


FIG. 3. (a) The optical image of the modified zone under the following conditions: pulse energy = $6 \mu J$, pulse repetition rate = 20 kHz, scanning speed = 1 mm/s, (b) The intensity distribution of peak 480 cm⁻¹, (c) 2D distribution of the percentage of the amorphous silicon, (d) log scale distribution of the amorphous

contrast in Fig. 3(a). Quantitative analysis at each pixel of the 2D mapping produces another 2D mapping, shown in Fig. 3(c), for the percentage of amorphous silicon in the modified zone. The 2D mapping is obtained by calculating the percentage of amorphous silicon at each pixel with the same method as described earlier and applied in Fig 2(b). Only a small number of pixels with relatively high amorphous silicon contents are visible in Fig. 3(c) because of the low value range on a linear scale. To better tell the small differences between pixels, the log scale distribution of the amorphous silicon is shown in Fig. 3(d). Each dot represents the value of log $[I_a/(I_a+I_c)]$ at the corresponding pixel. The highest percentage of amorphous silicon is found to be about 3% for this sample.

To better characterize the modification in terms of its structural changes, a TEM analysis is done. As illustrated in Fig. 4(a), one channel modification is written in the silicon wafer and a lamella is extracted along the x-z plane in the middle of the cross section of the modification. Figure 4(b) shows an SEM image of the cross-section of the channel along the x-y plane and the position of the lamella (in the yellow rectangular area). The channel modification is written with the pulse energy of $10 \,\mu$ J, pulse repetition rate of $20 \, \text{kHz}$, and scanning speed of $1 \, \text{mm/s}$. After removing

the surrounding materials by FIB with subsequent thinning, a lamella as shown in Fig. 4(c) is formed. The lamella is about $10 \times 10 \,\mu\text{m}^2$ in the x-z plane and about 100 nm thick in the y-direction. Figure 4(d) shows the SEM image of the lamella with more details. From Figs. 4(c) and 4(d), the lamella has been rotated (see the arrow). Figure 4(d) shows that the modifications are highly non-uniform. Pockets of severe modifications in dark color seem to appear in random locations against the lighter background, which is in its crystalline form. The long curly thin lines in the upper right corner and the faint line patterns in other areas are believed to be caused by micro strains. Some cracks can be found in the laser modified region, but it is believed that they are formed after thinning, due to the inherent stress distribution after laser writing. Figure 4(e) zooms in on one of the severely modified areas in the lamella. The laser modified region is also observed by highresolution transmission electron microscopy (HRTEM). Figure 4(f) is one example of the TEM results. The material in Fig. 4(f) is roughly divided into two parts. The upper part is mainly amorphous silicon and the lower part is mainly crystalline silicon. Figures 4(g) and 4(h) are HRTEM images of rectangular areas A and B in Fig. 4(f), respectively. Figure 4(g) clearly shows that the

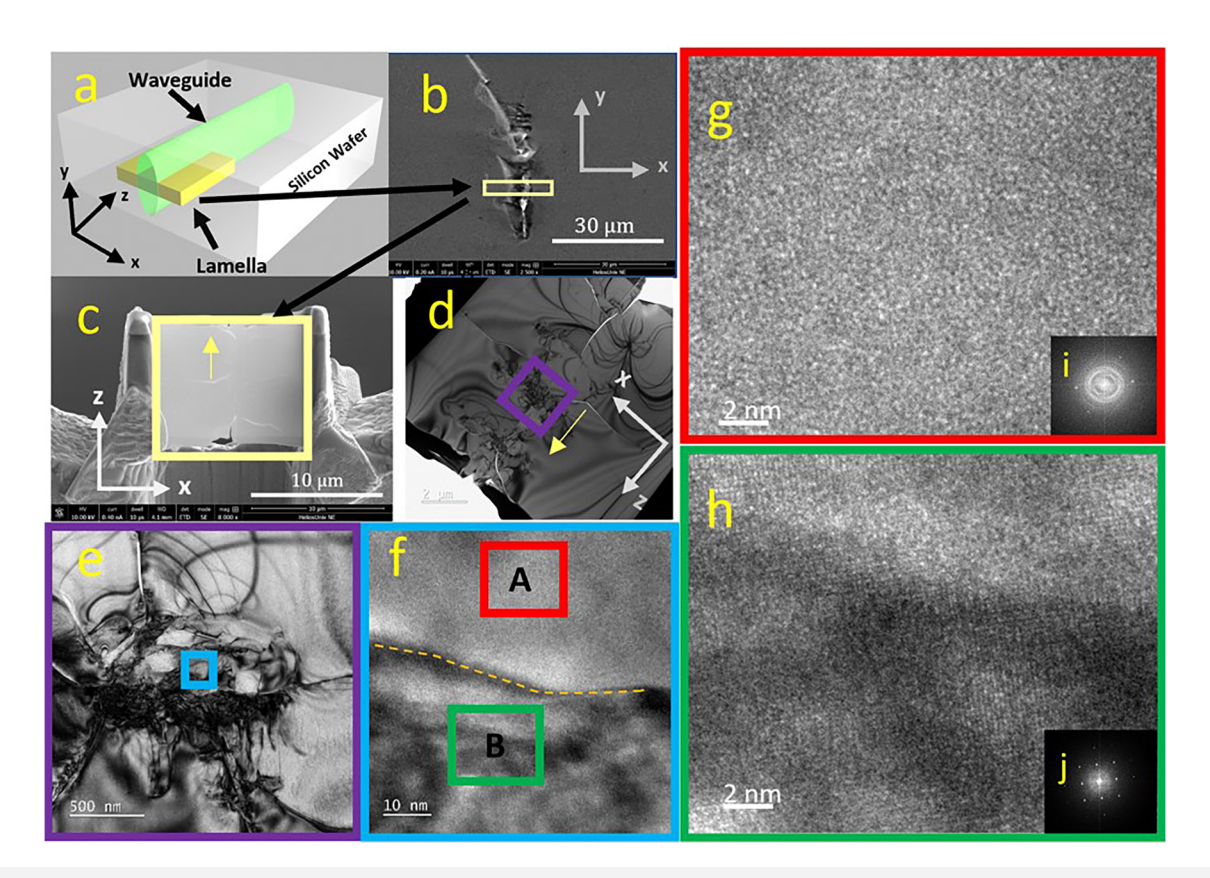


FIG. 4. (a) A 3D illustration to show the location of the lamella with respect to the channel modification written inside silicon. (b) The cross section of the channel and the location of the lamella (in the yellow box). (c) The lamella is analyzed by TEM. (d)–(f) The TEM image of the modification. (g) The HRTEM image of area A of (f) and its corresponding FFT [inset (i)]. (h) The HRTEM image of area B of (f) and its corresponding FFT [inset (j)].

silicon atoms are randomized. Figure 4(h) shows that the atoms are regular as the original crystalline silicon. The inset FFT images of i and j provide solid evidence for the above claim. For the first time, the HRTEM results directly show the appearance of amorphous silicon inside ns laser induced modifications.

The amorphous silicon is probably one reason for the light guiding ability of the channel since the refractive index of amorphous silicon is higher than that of monocrystalline silicon. However, it may not be the only reason, because the amorphous silicon in the modification is not uniform and the percentage is low

IV. CONCLUSIONS

We investigated the structural changes of ns laser induced modifications in bulk silicon. This analysis was performed by Raman microscopy and TEM. The measurements reveal a permanently induced transition from monocrystalline silicon to silicon with a disturbed crystal structure. The Raman results prove that the existence of amorphous silicon inside modifications and the percentage of the amorphous silicon were calculated based on the Raman spectrum. For the first time, the HRTEM images directly show the appearance of amorphous silicon inside nanosecond laser induced modifications. This may explain the origin of the positive refractive index change associated with the ns laser written channel modifications. It is believed that the amorphous silicon in combination with defects is responsible for a positive refractive index change in the range of 10⁻³. In addition, defects created in the modified zone serve as scattering sources for high losses of waveguides written inside silicon. To better understand the material change inside modifications, more experiments with different writing conditions are needed in the future. Our work is a step forward toward the goal of a single-step fabrication process of complicated waveguide structures in silicon. Meanwhile, our results show that future work is needed to write waveguides with more complicated shapes and better performance. We believe that a better understanding of the material changes inside laser induced modifications will inform future improvements.

ACKNOWLEDGMENTS

Financial support from the National Science Foundation (NSF) (Nos. 2128962, 1665456, and 2129006) and Air Force Office of Scientific Research (AFOSR) (No. FA9550-19-1-0078) is gratefully acknowledged. The authors thank the James R. Macdonald Laboratory of Kansas State University for their assistance.

AUTHOR DECLARATIONS

Conflict of Interest

The authors declare no conflicts of interest.

Author Contributions

Xinya Wang: Data curation (equal); Formal analysis (equal); Investigation (lead); Writing – original draft (lead). **Lanh Trinh:** Formal analysis (equal); Investigation (equal); Writing – review & editing (equal). **Xiaoming Yu:** Conceptualization (equal);

Supervision (equal); Writing – review & editing (equal). Matthew J. Berg: Supervision (equal); Writing – review & editing (supporting). Sajed Hosseini-Zavareh: Data curation (equal); Formal analysis (equal); Writing – review & editing (supporting). Brice Lacroix: Formal analysis (supporting); Resources (equal); Supervision (equal); Writing – review & editing (supporting). Pingping Chen: Data curation (supporting); Investigation (equal); Writing – review & editing (supporting); Investigation (equal); Writing – review & editing (supporting). Bai Cui: Formal analysis (supporting); Supervision (equal); Writing – review & editing (equal). Shuting Lei: Conceptualization (equal); Supervision (equal); Writing – review & editing (equal).

DATA AVAILABILITY

Data underlying the results presented in this paper are not publicly available at this time but may be obtained from the authors upon reasonable request.

REFERENCES

- ¹M. Beresna, M. Gecevičius, and P. G. Kazansky, "Ultrafast laser direct writing and nanostructuring in transparent materials," Adv. Opt. Photonics **6**, 293–339 (2014).
- ²H. Kämmer, G. Matthäus, K. A. Lammers, C. Vetter, M. Chambonneau, and S. Nolte, "Origin of waveguiding in ultrashort pulse structured silicon," Laser Photonics Rev. 13, 1800268 (2019).
- ³A. H. Nejadmalayeri, P. R. Herman, J. Burghoff, M. Will, S. Nolte, and A. Tünnermann, "Inscription of optical waveguides in crystalline silicon by midinfrared femtosecond laser pulses," Opt. Lett. **30**, 964–966 (2005).
- ⁴P. C. Verburg, G. R. B. E. Römer, and A. J. Huis in 't Veld, "Two-photon-induced internal modification of silicon by erbium-doped fiber laser," Opt. Express 22, 21958–21971 (2014).
- ⁵X. Yu, X. Wang, M. Chanal, C. A. Trallero-Herrero, D. Grojo, and S. Lei, internal modification of intrinsic and doped silicon using infrared nanosecond laser," Appl. Phys. A **122**, 1001 (2016).
- ⁶X. Wang, X. Yu, H. Shi, X. Xian, M. Chambonneau, D. Grojo, B. DePaola, M. Berg, and S. Lei, "Characterization and control of laser induced modification inside silicon," J. Laser Appl. 31, 022601 (2019).
- ⁷M. Chambonneau, X. Wang, X. Yu, Q. Li, D. Chaudanson, S. Lei, and D. Grojo, "Positive- and negative-tone structuring of crystalline silicon by laser-assisted chemical etching." Opt. Lett. 44, 1619 (2019).
- ⁸M. Chambonneau, Q. Li, M. Chanal, N. Sanner, and D. Grojo, "Writing waveguides inside monolithic crystalline silicon with nanosecond laser pulses," Opt. Lett. 41, 4875 (2016).
- ⁹G. Matthäus, H. Kämmer, K. A. Lammers, C. Vetter, W. Watanabe, and S. Nolte, "Inscription of silicon waveguides using picosecond pulses," Opt. Express 26, 24089–24097 (2018).
- 10 O. Tokel, A. Turnalı, G. Makey, P. Elahi, T. Çolakoğlu, E. Ergeçen, Ö. Yavuz, R. Hübner, M. Zolfaghari Borra, I. Pavlov, A. Bek, R. Turan, D. K. Kesim, S. Tozburun, S. Ilday, and F. Ö. Ilday, "In-chip microstructures and photonic devices fabricated by nonlinear laser lithography deep inside silicon," Nat. Photonics 11, 639–645 (2017).
- ¹¹I. Pavlov, O. Tokel, S. Pavlova, V. Kadan, G. Makey, A. Turnali, Ö. Yavuz, and F. Ö. Ilday, "Femtosecond laser written waveguides deep inside silicon," Opt. Lett. 42, 3028–3031 (2017).
- ¹²M. Chanal, V. Y. Fedorov, M. Chambonneau, R. Clady, S. Tzortzakis, and D. Grojo, "Crossing the threshold of ultrafast laser writing in bulk silicon," Nat. Commun. 8, 773 (2017).
- ¹³A. Turnali, M. Han, and O. Tokel, "Laser-written depressed-cladding wave-guides deep inside bulk silicon," J. Opt. Soc. Am. B 36, 966–970 (2019).

- ¹⁴X. Wang, X. Yu, M. Berg, B. DePaola, H. Shi, P. Chen, L. Xue, X. Chang, and S. Lei, "Nanosecond laser writing of straight and curved waveguides in silicon with shaped beams," J. Laser Appl. 32, 022002 (2020).
 ¹⁵X. Wang, X. Yu, M. Berg, P. Chen, B. Lacroix, S. Fathpour, and S. Lei, "Curved
- ¹⁵X. Wang, X. Yu, M. Berg, P. Chen, B. Lacroix, S. Fathpour, and S. Lei, "Curved waveguides in silicon written by a shaped laser beam," Opt. Express 29, 14201–14207 (2021).
- ¹⁶H. Iwata, D. Kawaguchi, and H. Saka, "Electron microscopy of voids in Si formed by permeable pulse laser irradiation," Microscopy 66, 328–336 (2017).
- ¹⁷K. Shimamura, J. Okuma, S. Ohmura, and F. Shimojo, "Molecular-dynamics study of void-formation inside silicon wafers in stealth dicing," J. Phys.: Conf. Ser. 402, 012044 (2012).
- ¹⁸H. Iwata, D. Kawaguchi, and H. Saka, "Crystal structures of high-pressure phases formed in Si by laser irradiation," Microscopy 67, 30–36 (2018).
 ¹⁹H. Saka, H. Iwata, and D. Kawaguchi, "Thermal stability of laser-induced
- ¹⁹H. Saka, H. Iwata, and D. Kawaguchi, "Thermal stability of laser-induced modified volumes in Si as studied by *in situ* and *ex situ* heating experiments," Microscopy **67**, 112–120 (2018).
- 20 M. Chambonneau, D. Grojo, O. Tokel, F. Ö. Ilday, S. Tzortzakis, and S. Nolte, "In-volume laser direct writing of silicon—Challenges and opportunities," Laser Photonics Rev. 15, 2100140 (2021).

- ²¹V. G. Golubev, V. Y. Davydov, A. V. Medvedev, A. B. Pevtsov, and N. A. Feoktistov, "Raman scattering spectra and electrical conductivity of thin silicon films with a mixed amorphous-nanocrystalline phase composition: Determination of the nanocrystalline volume fraction," Phys. Solid State 39, 1197–1201 (1997).
- ²²M. Newville, S. Till, B. A. Daniel, R. Michal, I. Antonino, and N. Andrew (2016). "Lmfit: Non-linear least-square minimization and curve-fitting for Python," Astrophysics Source Code Library. https://ascl.net/1606.014.
- 25S. Hosseini-Zavareh, R. Luder, M. Thirugnanasambandam, H. W. Kushan Weerasinghe, B. R. Washburn, and K. L. Corwin, "Fabrication and characterization of short acetylene-filled photonic microcells," Appl. Opt. 58, 2809–2816 (2019).
- ²⁴S. Hosseini-Zavareh, M. Thirugnanasambandam, H. W. Kushan Weerasinghe, B. R. Washburn, and K. L. Corwin, "Improved acetylene-filled photonic bandgap fiber cells fabricated using a tapering method," in *Frontiers in Optics* (Optical Society of America, Washington, DC, 2018), p. JW4A-95.
- ²⁵R. J. Luder, S. Hosseini-Zavareh, C. Wang, M. Thirugnanasambandam, B. R. Washburn, and K. L. Corwin, "Short acetylene-filled photonic bandgap fiber cells toward practical industry standards," in *Conference on Lasers and Electro-Optics*, OSA Technical Digest, San Jose, CA, 5–10 June 2016 (Optica Publishing Group, Washington, DC, 2016).